

Diffusion of metals in geosynthetic clay liners

K. Lange¹, R. K. Rowe² and H. Jamieson³

¹Graduate Student, GeoEngineering Centre at Queen's-RMC, Queen's University, Kingston, Ontario, Canada K7L 3N6, Telephone: +1 613 533 6000 (78227), Telefax: +1 613 533 2128, E-mail: lange@ce.queensu.ca

²Professor, GeoEngineering Centre at Queen's-RMC, Queen's University, Kingston, Ontario, Canada K7L 3N6, Telephone: +1 613 533 6933, Telefax: +1 613 533 6934, E-mail: kerry@ce.queensu.ca

³Associate Professor, GeoEngineering Centre at Queen's-RMC, Queen's University, Kingston, Ontario, Canada K7L 3N6, Telephone: +1 613 533 6181, Telefax: +1 613 533 6592, E-mail: jamieson@geol.queensu.ca

Received 4 February 2008, revised 22 October 2008, accepted 22 October 2008

ABSTRACT: The potential for using geosynthetic clay liners (GCLs) to mitigate metal mobility is dependent, in part, on consideration of its effectiveness as a diffusive barrier. In this context, laboratory-measured diffusion coefficients and supporting sorption data for metals (Al, As, Cd, Cu, Fe, K, Mg, Mn, Ni, Sr, Zn) are reported for the following four cases where a GCL might serve as an effective barrier material to metals and metalloids: acidic rock drainage, gold mine tailings, lime-treated mine effluent, and municipal solid waste. The average diffusion coefficients for Cu, Cd, Zn, Fe and Ni covered a narrow range from 0.67×10^{-10} to 0.89×10^{-10} m²/s. The diffusion coefficients for As, Al, Mg, Mn and Sr were in the range $D = 0.80 \times 10^{-10}$ to $D = 1.6 \times 10^{-10}$. The diffusive movement of other more common inorganic ions such as Ca, Na, S (SO₄) and Cl are also considered, as well as the impact of pH, Eh and speciation on metal mobility in GCLs.

KEYWORDS: Geosynthetics, Geosynthetic clay liners (GCL), Metals, Bentonite, Diffusion, Sorption, Tailings

REFERENCE: Lange, K., Rowe, R. K. & Jamieson, H. (2009). Diffusion of metals in geosynthetic clay liners. *Geosynthetics International*, 16, No. 1, 11–27. [doi: 10.1680/gein.2009.16.1.11]

1. INTRODUCTION

Concerns related to metal pollution continue to increase worldwide. Accumulation of potentially hazardous metals is of great concern since, contrary to organic xenobiotic compounds, they are not subject to any degradation (Bourg 1995). Plants have a tolerance to grow in contaminated soils, and owing to the accumulation of high amounts of metals (sometimes extremely high: e.g. Bourg 1995), they can become a polluted link in the food chain. Among the eight highest-priority sources of contaminants that threaten public groundwater systems identified by Knox and Canter (1996) were sources designed to store, treat and dispose of substances including industrial and municipal landfills, hazardous waste sites, mine tailings and mine waste piles. In the mining industry, even if greater use is made of waste utilisation and alternative waste disposal methods, the greatest portion of mining wastes will still be disposed of in land disposal facilities such as waste piles, tailings ponds, and settlings impoundments (Merian 1991).

Considerable research has been devoted to examining the use of geosynthetic clay liners (GCLs) for landfill applications (e.g. Rowe *et al.* 2004; Barroso *et al.* 2006;

Bouazza and Vangpaisal 2006, 2007; Dickinson and Brachman 2006; Saidi *et al.* 2006; Touze-Foltz *et al.* 2006; Touze-Foltz and Barroso 2006; Southen and Rowe 2007; Bouazza *et al.* 2007; Take *et al.* 2007; Müller *et al.* 2008), and they are now slowly being introduced into the mining sector (e.g. Olsta and Friedman 2002), where metal-rich leachates are typically encountered. There is a need for low-cost, readily available materials that can adsorb metal ions efficiently. The interest in GCLs has prompted a number of studies to examine their engineering behaviour (hydraulic conductivity, swell index) in the presence of salt solutions and municipal solid waste (MSW) leachates (e.g. Kolstad *et al.* 2004; Rowe *et al.* 2004; Katsumi *et al.* 2008). However, the transport of metals in GCLs from waste leachates, especially related to mining, has received little attention in the literature. Recent work by Lange *et al.* (2007a) quantified the advective movement of two synthetic mining waters through a GCL; delayed breakthrough curves for all metals demonstrated the strong retention capacity of the bentonite in the GCL tested.

Provided that there is adequate drainage, so that large hydraulic heads do not develop over the liner, contaminant

migration in low-permeability barrier materials is often dominated by diffusion (Rowe *et al.* 2004). Contaminant transport modelling requires the input of a diffusion coefficient. Short-term (laboratory) diffusion tests, using similar material and solutions to those found in the field, have been shown to ably explain field-scale diffusive migration (e.g. Rowe *et al.* 2004; Rowe and Booker 2005). Diffusion coefficients in GCLs for Cl and Na have been measured by Lake and Rowe (2000) and for Al by Lake *et al.* (2007). However, there are currently no reported diffusion coefficients for metals such as As, Ni and Zn in GCLs.

Effective diffusion coefficients for Cl have been documented for different clay soils (e.g. Barone *et al.* 1990; Kozaki *et al.* 1998; Rowe *et al.* 2004) and typically span a range from 1.5×10^{-10} to 10×10^{-10} m²/s. Some metal diffusion coefficients have also been reported for clay and clay mixtures, and tend to range from 1.0×10^{-10} to 3×10^{-10} m²/s (e.g. Do and Lee 2006). Rowe *et al.* (2004) discuss how the effective diffusion coefficient can incorporate factors including tortuosity, osmotic flow, electrical imbalance and, in some cases, anion exclusion. Expressions quantifying the diffusion coefficient of an ionic species at infinite dilution (e.g. Nernst) have been derived on the basis of factors such as the mobility, mass and radius of the diffusing ions, and the properties of the liquid, such as viscosity, dielectric constant and temperature (Reddi and Inyang 2000). In reporting mutual diffusion coefficients in different aqueous electrolyte solutions, Lobo and Quaresma (1990) show how diffusion changes among differing species. For example, the Cd aqueous diffusion coefficient for a 0.1 M solution of CdCl₂ (9.0×10^{-10} m²/s) was 1.7 times greater than that for a 0.1 M solution of CdSO₄ (5.2×10^{-10} m²/s).

Lake and Rowe (2000) measured Na and Cl diffusive migration in GCLs and examined how different source solutions and voids ratios affected diffusion (Na: 0.35×10^{-10} to 3.0×10^{-10} m²/s and Cl: 0.35×10^{-10} to 3.0×10^{-10} m²/s for porosities ranging from 0.56 to 0.80). Their findings highlighted the need for caution in using published aqueous (infinite dilution) diffusion coefficients for field conditions, because the measured soil diffusion coefficients are really mass transfer coefficients that incorporate the many factors mentioned by Rowe *et al.* (2004), as noted above. Lake and Rowe (2000) found that Na and Cl ions moved at different rates in diffusion tests than would be expected based on diffusion coefficients in free solution at infinite dilution. This was attributed to the effect of backward diffusion of SO₄ ions (into the source reservoir) and the higher gradient of Cl relative to Na owing to the initial presence of Na ions in the receptor reservoir (diffused from GCL during hydration). Chloride ions pulled the partner Na ions through the GCL in order to maintain electroneutrality, which in turn caused the Na diffusion coefficient to increase, and that of Cl to decrease. It is the summed effect of the ion-pair dipoles in the solution that creates the macroscopic 'diffusion potential' that is typically measured (Jungnickel *et al.* 2004). Therefore, if the partner ion in the ion pair is changed (or if other ions are added to solution), then a

different diffusion coefficient may be observed. Notably, Lake and Rowe (2000) observed a 50% increase in the Cl diffusion coefficient when the source was changed from an NaCl salt solution to a synthetic MSW leachate. They hypothesised that 'the deviation of the Cl results were [sic] influenced more by the complex interaction of varying gradients for the leachate than a decrease in effective pore space due to double layer contraction'. Similarly, research by Jungnickel *et al.* (2004) using a finite element solution for the complete set of equations governing coupled multi-ion reactive transport reinforced the observation that the diffusion coefficients back-calculated from a standard diffusion analysis represent system-specific mass transfer coefficients, and should be extrapolated to new systems, again with caution. Sorption can change the geochemistry of the system, as the ion pair will change when one ion is sorbed, causing counter-ions to maintain electroneutrality (commonly found in the pore solution) (Jungnickel *et al.* 2004).

Questions that concern metal interactions with GCLs are often answered using the data from sorption experiments with similar montmorillonite clay. Such metal 'accounting' information is often performed using single or equimolar multi-metal permeants and, for analytical limitations or ease of measurement, often uses metal concentrations that are much larger than actual field values (e.g. Merian 1991). Application of these data to a landfill or mine tailings model may raise some concern, as multiple metal ions in the solution will 'yield unanticipated chemical combinations because of the synergetic and antagonistic effects that they exert on each other' (Kaoser *et al.* 2005). In multi-metal solutions, metal sorption often increases with decreasing ionic strengths, or less competing species.

Hydrolysis and complexation tend to increase the solubility of metals, while the precipitation and adsorption will delay the metal availability and transport (Bourg 1995). Doner (1978) noted that Cl can be an efficient inorganic complex former at high concentrations of Cl (e.g. > 0.01 M Cl), causing the solubilisation of metals. For example, Schuster (1991) showed that some Hg in a soil could be mobilised by complexing with Cl and OH. Since the solubility of HgCl₂ and Hg(OH)₂ is rather high, Hg had an affinity to these ligands, which led to an increased mobility. Natural organics and synthetic multidentate chelators are also very powerful complex formers. For example, the concentration of dissolved organic carbon (DOC) in municipal waste leachates is one of the most important factors involved in the solubilisation and subsequent migration of metals through soils (Frost and Griffin 1977; Artiola-Fortuny and Fuller 1982).

It is widely recognised that it is not that the total amount or concentration of a given metal is most important for understanding its environmental behaviour, but rather that the key to the flux of a metallic element is its speciation (Bourg 1995). As it is difficult, analytically, to identify the various solute species present in solution, equilibrium modelling is typically employed. Thermodynamic computer programs such as PHREEQC

(Parkhurst and Appelo 1999) can estimate the presence of different species in solution, and can use a solubility approach to evaluate likely precipitates.

To this end, the current study investigated the diffusive transport and sorption of metals in GCLs present in quantities and solutions similar to those reported at actual field sites. Diffusion was measured from four solution matrices that represented cases where a GCL might serve as an effective barrier material. The solutions considered were: acidic rock drainage, water from gold mine tailings, lime-treated acidic rock drainage, and landfill leachate with metal loading. The primary objectives of this research were:

1. to estimate the diffusion coefficients of 12 elements, including key contaminant metals (Cu, As) and other anions (Cl, SO₄), in GCLs by using a numerical model to quantify physical laboratory data;
2. to clarify the diffusion coefficient's dependence on solution composition.

Geochemical data, including the measurement of ancillary ions, and speciation modelling help to explain observed phenomena.

2. EXPERIMENTAL: METHODS AND MATERIALS

The Bentofix NWL GCL tested in this study was provided by Terrafix Geosynthetics Inc. and is made up of a nonwoven carrier geotextile, a layer of granular Wyoming sodium bentonite, and a nonwoven cover geotextile needle-punched together with the fibres thermally treated on the carrier geotextile. X-ray diffraction analysis of the bulk material and clay fraction (< 4 µm) was performed using a Rigaku automated powder diffractometer equipped with a copper X-ray source (40 kV, 35 mA) and a scintillation X-ray detector. Quantitative analyses of the diffraction data (using integrated peak areas and reference intensity ratios) provided the following analysis of the GCL bentonite: 77% smectite; 8% plagioclase; approximately 5% each of cristobalite and quartz; and trace amounts of illite, mica, calcite, pyrite and clinoptilolite (a zeolite). The presence of feldspar, quartz, cristobalite, mica and calcite is consistent with previous characterisation of the GCL using micro-X-ray diffraction (Lange *et al.* 2007b). The predominant inorganic ions in the porewater based on the volume of water present at saturation were Na (270 mg/L), Ca (18 mg/L), Mg (4.0 mg/L), K (6.2 mg/L), SO₄ (380 mg/L) and Cl (29 mg/L). The total cation exchange capacity of the bentonite measured 91 meq/100 g (EPA method 9081), and the average mass of bentonite per unit area of GCL was 4.24 kg/m².

The chemical composition of the contaminated waters used for this study is given in Table 1. Acidic rock drainage (ARD) is a well-known environmental problem that occurs when water comes into contact with pyrite (and other sulphide minerals) in oxidising conditions and produces acidic water, often resulting in high dissolved metal content. The ARD solution used in this study is

Table 1. Chemical composition of synthetic mine and landfill waters

	ARD	GMW	LL	TARD
Al	80	5	10	12
As	2.5	5.4	1	1
Ca	4.6	117	700	365
Cd	45	7	2	12
Cu	15	–	1	2
Fe	200	1.5	12	10
K	400	12	190	8
Mn	23	1.7	7	7
Mg	1	60	244	45
Na	800	776	2300	340
Ni	17	–	6	6
Sr	–	2	12	–
Zn	102	–	16	8
SO ₄	3102	1506	75	1290
Cl	2000	1000	6000	1000
NH ₄	–	6	413	–
PO ₄	–	–	16	–
NO ₃	–	6	29	–
Urea CO(NH ₂)	–	–	300	–
HCO ₃ + CO ₃	–	310	3111	–
Acetic acid	–	–	7343	–
Propionic acid	–	–	4965	–
Butyric acid	–	–	959	–
pH	2.6	6.8	5.4	5.8
Eh	388	198	80	154

Units: Concentrations = mg/L; pH = pH units; Eh = mV.

similar to that described in Lange *et al.* (2007a). The second solution represents a pH-neutral water with elevated As, typical of those associated with carbonate-associated gold mine tailings and based on tailings porewaters sampled by Walker (2006, oral correspondence). The final mine-related solution is ARD water that had been treated with lime, similar to that which is likely to be found in a polishing pond (hereafter referred to as TARD for 'treated' ARD). Allan (1995) stated that 'water losses and water gains at a typical metal mine show that the main direct release of metals to freshwaters is from tailings and polishing ponds and emission later in the beneficiation stage.' One solution was modelled after a landfill leachate (LL) during the 'early anaerobic degradation phase I, II' (Farquhar and Rovers 1973), where acid fermentation (and CO₂ production) causes a decrease in pH, oxygen is being consumed, and metal mobility is likely to be highest (Uruse *et al.* 1997). ARD, GMW and LL waters were synthesised in the laboratory using analytical-grade salts, and the TARD was provided by CANMET Laboratories (Mining and Mineral Sciences, Ottawa), and spiked with metals to simulate conditions similar to a treated ARD found in Feng *et al.* (2000). Figure 1 shows the Eh and pH conditions of the waters in comparison with other leachates and natural waters.

The distribution of aqueous species for the waters and the thermodynamic potential for minerals (salts) to precipitate from solution, expressed in terms of a saturation index (SI), were calculated using PHREEQC Interactive version 2.13.2 (Parkhurst and Appelo 1999), with the Minteq v4 database: measured aqueous metal concentra-

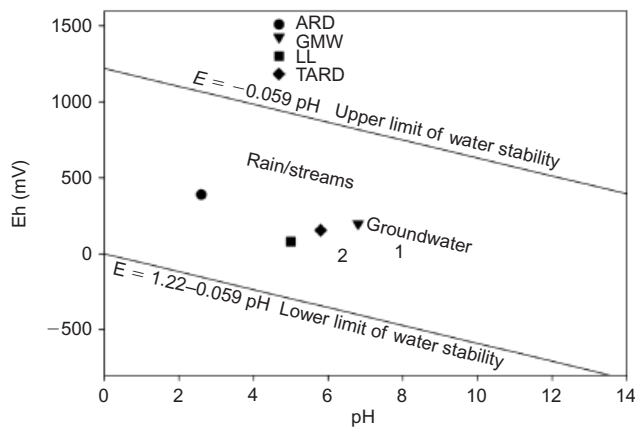


Figure 1. Eh–pH diagram showing conditions for LL, ARD, GMW and TARD, compared with selected natural and industrial waters (modified from Baas-Becking *et al.* 1960; Brookins 1988). 1, MSW, Osaka (Zhang *et al.* 2004); 2, Dupage MSW (Griffin and Shrimp 1976)

tions were input in mg/L; pe was calculated from measured Eh; alkalinity was input as the sum of all carbonate species; and the organic acids were incorporated by inputting the amount of dissociated acetate, propionate and butyrate ion concentrations calculated from their respective K_a (weak acid ionisation constant) values.

2.1. Diffusion tests

The double reservoir diffusion test cell was modified from Lake and Rowe (2000), and consisted of a cylindrical glass apparatus 70 mm in diameter and 80 mm high. Glass was tolerant of acidic conditions, and ensured no reactions with metals. The top or source reservoir was separated from the bottom reservoir (receptor) by a hydrated GCL. The GCL was cut using a water-wetted steel circular cutting tool, and weighed to ensure a constant mass per unit area for samples tested in the different cells. Each reservoir was sealed with a glass plate and silicone; a small port allowed for injection and removal of liquid using 1 mL syringes. A small hole was cored in the top plate of the source reservoir and sealed with Teflon tape. This hole was used to place a pH, Eh and Cl electrode directly into the source solution. Spacers were adjusted above and below the GCL to ensure swelling to a specified height ($H = 13$ mm for this study). A 6 mm porous disc and filter paper encapsulated the GCL on both sides, which ensured even swelling, and prevented soil particles from entering the reservoirs (i.e. filtering). The GCL was hydrated using deionised, deaired water (DDW) from below the sample, under a small head (~ 20 mm) for 5 days. After the GCL was hydrated, 50 mL of DDW was placed above the sample. Chloride, SO_4 , pH (in the source reservoir), Mg, Ca and Na were measured, and once equilibrium was reached (i.e. same concentrations in both reservoirs) after one month, the top reservoir was filled with solution (e.g. ARD, GMW, LL or TARD) with initial concentrations as given in Table 1. The DDW remained in the receptor. Previous testing and knowledge of key

transport times (by the authors) allowed minimal sampling for the current study: 1 mL of sample was withdrawn every 3 days (or 0.33 mL/day) from both the source and receptor and replaced by the equivalent amount of DDW. Chemical analysis measured 24 cationic elements (using an inductively coupled plasma optical emission spectrometer: Varian, AX-Vista Pro CCD Simultaneous ICP-OES). Cl, pH and Eh were measured by an ion-specific electrode. Sulphate was calculated based on total S (S was assumed to be fully oxidised). The results from the source and receptor concentrations in eight test cells (i.e. tests for each source water were duplicated) were used, together with the porewater concentrations at the termination of tests after 40 days, to establish the diffusion and sorption parameters reported herein.

Chemical transport over time from the source to receptor reservoir is governed by

$$n \frac{\partial c}{\partial t} = - \frac{\partial f_T(t)}{\partial z} - \rho K_d \frac{\partial c}{\partial t} \quad (1)$$

where n is the soil porosity [$L^3 L^{-3}$], c is the solute concentration in the solution phase [ML^{-3}], t is time [T], z is the distance from the contaminant source [L], K_d is the distribution coefficient of the solute [$L^3 M^{-1}$], ρ is the dry density of the soil [ML^{-3}], and $f_T(t)$ is the mass flux of contaminant into the clay at time t [$ML^{-2}T^{-1}$], which for the case with zero Darcy flux (as in these tests) is given by

$$f_T(t) = -nD \frac{\partial c(t)}{\partial z} \quad (2)$$

where D is the diffusion coefficient. The boundary condition for both the source and receptor reservoirs is of the finite mass type (Rowe *et al.* 2004). For the source compartment, the concentration at any time, $c(t)$, is given by

$$c_T(t) = c_{s0} - \frac{1}{H_r} \int_0^t f_T(t) dt - \frac{q_c}{H_r} \int_0^t c_t(t) dt \quad (3)$$

where c_{s0} is the initial contaminant concentration in the source solution [ML^{-3}]; H_r is the volume of source fluid per unit area of sample (i.e. typically the height of the fluid in the reservoir) [L]; and q_c is the amount of fluid withdrawn from the source reservoir per unit area of the sample [LT^{-1}] and replaced by DDW (this term is used to account for the mass loss in fluid collected for sampling).

Similarly, the receptor concentration at any time, $c_B(t)$, is given by

$$c_B(t) = c_{r0} + \frac{1}{h_b} \int_0^t f_b(t) dt - \frac{q_c}{h_b} \int_0^t c_b(t) dt \quad (4)$$

where c_{r0} is the initial contaminant concentration in the receptor solution [ML^{-3}]; h_b is the volume of receptor fluid per unit area of sample (typically the height of the receptor reservoir) [L]; $f_b(t)$ is the mass flux of contaminant into the receptor at time t [$ML^{-2}T^{-1}$]; and q_c is the amount of sample withdrawn from the receptor reservoir per unit area of the sample [LT^{-1}].

The diffusion coefficient for soils is commonly reported as the product of the effective diffusion coefficient D_e

[$L^2 T^{-1}$] and effective porosity n_e . The effective porosity is typically lower than total porosity (n), and is an important parameter describing accessible transport pathways, especially when accounting for anionic species that may experience anion exclusion. Lake and Rowe (2000) reported diffusion coefficients based on the total porosity, that is, $D_p = nD$. They showed that for a thin soil layer such as the GCL, the precise values of n_e and D_e were not critical to predicting transport, provided that the values of n_e and D_e corresponded to the same product $D_e n_e = D_p$. Lake and Rowe (2000) showed how the total porosity was sufficient for modelling contaminant migration in GCLs. This approach of using D_p was convenient, since generally only the total porosity n_t is known for a GCL, and the effective porosity n_e may vary from one contaminant to another.

Upon completion of the diffusion test, the porewater and soil fraction of the GCL's bentonite was analysed for 24 cationic elements (ICP-OES), Cl, SO_4 , pH, and Eh (similar to above). Porewater was measured by shaking the wet GCL bentonite with DDW using a mechanical shaker (time = 2 h) at a liquid to solid ratio of 10:1, followed by centrifugation and filtration. Soil digestion was performed by aqua regia (Chen and Ma 2001), and cation content was reported in micrograms per gram of soil. The governing differential equation (Equation 1) for diffusive transport was solved subject to these boundary conditions (Equations 2–4) using POLLUTE v7 (Rowe and Booker 2005), and the diffusion and sorption parameters (D and K_d) were adjusted to obtain a best fit to the concentration–time data in the source and receptor and the porewater concentrations at the termination of the tests.

2.2. Batch sorption tests

The sorption by the GCL bentonite for each type of water was determined by equilibrating 0.05–2 g of clay with 65 mL of solution in 100 mL capped flasks followed by continuous shaking on a table rotary shaker (22°C) for 24 h. The equilibrium pH, Eh and Cl values were recorded periodically, and at termination the suspension was filtered and duplicate measurements of the supernatant were chemically analysed (24 cationic elements by ICP-OES). Typically, sorption tests will adjust the pH to a constant value; however, the authors did not want to alter the original solution composition. This allowed observation of the natural pH increase of the solution in contact with the bentonite, which was typically about 1–2 units above the initial pH. The difference between the initial elemental concentration and the equilibrium (final) concentration (C_e) was used to compute the amount of element removal. Isotherms were constructed from the data by plotting the amount of constituent removed from solution per gram of bentonite (Q_e) on the y axis and C_e on the x axis. Sorption kinetic tests showed some metals undergoing significant sorption within the first hour, but by the 24 h mark all concentrations and pH had stabilised. Based on these kinetic studies, the 24 h batch test was deemed acceptable. Sorption was reported by the distribution coefficient K_d [$L^3 M^{-1}$], which often incorporates a combination of adsorption/desorption, precipitation/dissolution and complexation reactions.

3. RESULTS AND DISCUSSION

3.1. Diffusion experimental results and analysis

The diffusion coefficients of metals and other inorganic ions were determined from calibration of the numerical model to

1. the concentration–time data and
2. the average porewater concentration at test termination.

Diffusion was modelled using a layered scheme, which consisted of an upper porous disc, top geotextile fabric, bentonite soil, bottom geotextile fabric, and lower porous disc. Calculations were based on the GCL height (13 mm) and total porosity n (0.80–0.83), measured at the end of the test (40 days).

For retarded or sorbed species, an approximation to the bulk partition coefficient, termed K_d , was calculated from the soil concentration (C_s) and respective porewater concentration (C_{aq}) at test termination, based on

$$K_d = \frac{C_s}{C_{aq}} \quad (5)$$

This assumed that a local equilibrium was reached between the soil and the porewater at the end of the test (similar to Do and Lee 2006). In some cases K_d was slightly altered from this value to achieve a better fit to the data. For example, the K_d value of 43 mL/g was calculated from the C_s and C_{aq} measured for Cd (in TARD) of 0.081 mg/g (of soil) and 1.89 mg/L, respectively; this K_d value was decreased to 38 mL/g to provide a better fit to the data. The reason for this alteration could be that one porewater value (i.e. average) was extracted for the entire depth of the GCL owing to material limitations, yet the concentrations of attenuated metals, as shown in Lange *et al.* (2007a), typically vary by location within the GCL.

Figures 2 to 5 show Zn, Ni, Cu and Cd concentration profiles over time plotted in terms of normalised concentration (c/c_0). Single data points reflect the experimentally measured values, and the solid lines represent the model (Pollute) results. At 40 days, the experiment was terminated as certain metals began to undergo a sudden faster rate of decline in the source reservoir starting as early as 35 days, as is evident by the Zn (TARD) curve shown in Figure 2. An increase of Zn concentration in the receptor reservoir was not measured, however, which suggests that a different retention mechanism within the GCL may be operative: this is the subject of a separate study. In such cases, the best-fit line to the data was achieved using a 'fit by eye' approach instead of the least squares method, to prevent these last data points from affecting the overall trend.

The diffusion characteristics of the metals investigated are quite similar in many respects, and the following conclusions can be drawn from the comparison between diffusion profiles, some of which are shown in Figures 2 to 5.

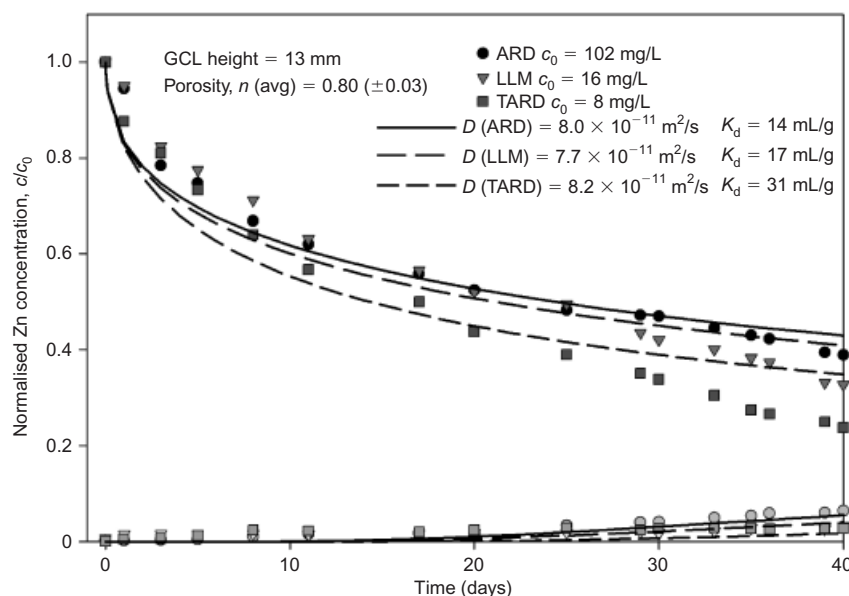


Figure 2. Source and receptor diffusion profiles of Zn for various solutions. Symbols represent the measured concentrations, and lines give the calculated profiles. Closed symbols represent source values, and open symbols show the receptor values

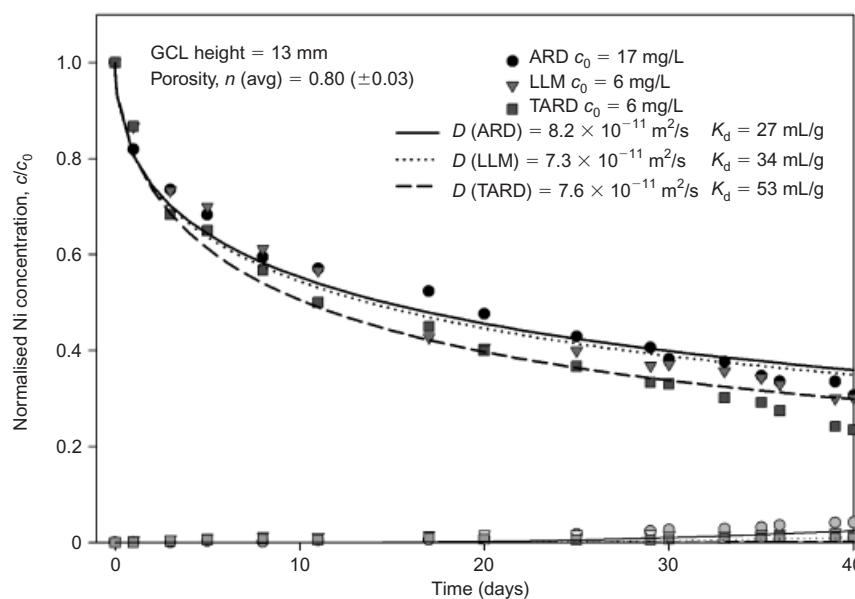


Figure 3. Source and receptor diffusion profiles of Ni for various waters. Symbols represent the measured concentrations, and lines give the calculated profiles. Closed symbols represent source values, and open symbols show the receptor values

1. The source concentration exhibited a steady decline as the metal diffused into the GCL and was diluted through sampling (replacement of removed sample with water).
2. The receptor concentration tended to remain very low, typically under $c/c_0 < 0.1$ for the duration of the test. These results imply that the metals were significantly retarded within the GCL.
3. The modelled diffusion coefficients for each metal from different solutions are very close to one another. The coefficients for Ni (Figure 3) ranged from $0.73 \times 10^{-10} \text{ m}^2/\text{s}$ to $0.82 \times 10^{-10} \text{ m}^2/\text{s}$ (average of $0.77 \times 10^{-10} \text{ m}^2/\text{s}$). This suggests that

solution composition has some effect on the metal diffusion coefficient; however, sorption to the GCL was the dominant control on metal mobility. As discussed more fully in a later section, this was not the case for other ions such as Na and Ca, where solution composition and pH had a significant impact on their diffusive migration.

In some instances, a precipitate formed, thus limiting metal mobility. Copper from TARD waters, for example, showed a very sharp decline (Figure 4), and modelling of diffusion was impossible, even using high sorption coefficients. Equilibrium modelling showed that copper

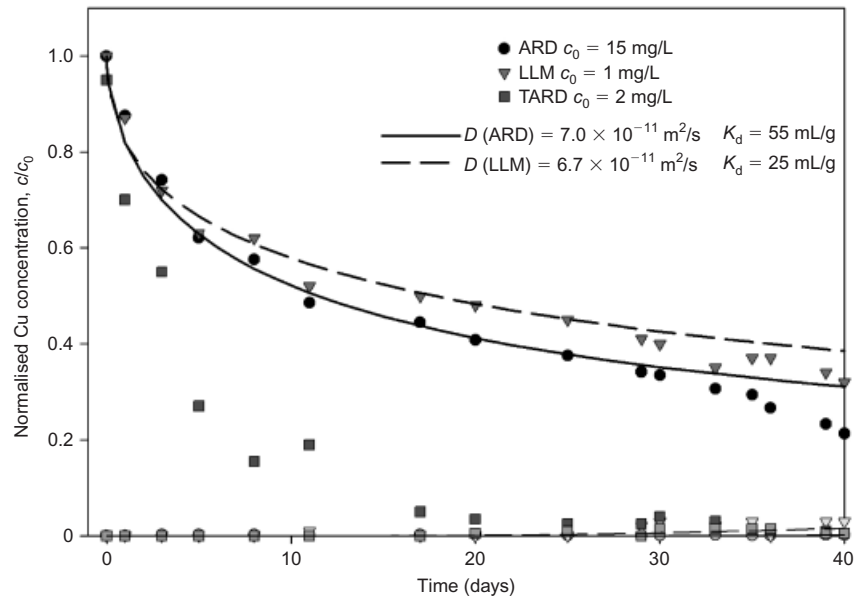


Figure 4. Source and receptor diffusion profiles of Cu for various solutions. Symbols represent the measured concentrations, and lines give the calculated profiles. Closed symbols represent source values, and open symbols show the receptor values

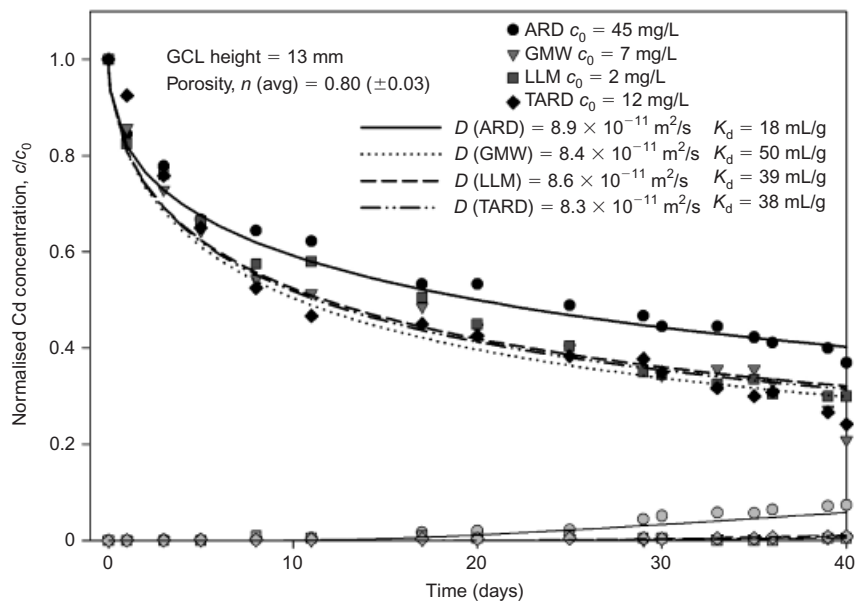


Figure 5. Source and receptor diffusion profiles of Cd for various solutions. Symbols represent the measured concentrations, and lines give the calculated profiles. Closed symbols represent source values, and open symbols show the receptor values

hydroxide ($\text{Cu}(\text{OH})_2$) and copper sulphate (CuSO_4) had saturation indices close to 1 and therefore may have precipitated when in contact with the OH and SO_4 ions from the bentonite porewater (pH \sim 8). The mass balance (at test termination) of Cu for the TARD experiment showed that only 78% of the original Cu mass was recovered: in such cases it is the authors' experience that the remaining mass tends to precipitate in the surface of the GCL fabric.

Most metals associated with the ARD water tended to have higher diffusion coefficients and showed higher concentrations over time in the receptor reservoir. The positive charge that develops at the clay surface in an

acidic medium can result in positive ions being repelled from some surfaces, analogous to the effect of 'anion exclusion', where ionic movement becomes accelerated (Rowe *et al.* 2004). The migration of Cd in ARD was very different from that of the three other solutions shown in Figure 5. All waters had similar diffusion coefficients, but the acidic pH (and possibly the high concentration) of Cd in the ARD water yielded a much lower K_d and a larger concentration in the source and receptor.

The summarised results from the diffusion tests for the four waters (ARD, GMW, LL and TARD) are reported in Table 2. The total mass retained (column 5) refers to the

Table 2. Effective diffusion coefficients and measured data from diffusion testing and data from 24 h batch sorption experiments.

	(1) Initial concentration, C_0 (mg/L)	(2) Diffusion coefficient, D (m ² /s)	(3) Porewater concentration, C_{aq} (mg/L)	(4) Linear distribution coefficient, K_d (diffusion) (mL/g)	(5) Total mass retained in GCL (mg)	(6) Distribution coefficient, K(batch) (mL/g)	(7) Freundlich constant, ϵ	(8) Regression coefficient, R^2
Aluminium Al ^a								
ARD	80	1.6×10^{-10}	24.1	15	6.63	100	0.6	0.95
GMW	5	r	10.3	–	–0.60	31	0.7	0.96
LL	10	r	10.7	–	–0.27	12	1	0.95
TARD	12	r	11.3	–	–0.70	17	1	0.95
Arsenic As								
ARD	2.5	1.3×10^{-10}	0.8	5.5	0.11	68	1	0.96
GMW	5.4	0.80×10^{-10}	1.4	5	0.15	13	1	0.91
LL	1.0	0.86×10^{-10}	0.5	2	0.05	20	0.9	0.90
TARD	1.0	0.88×10^{-10}	<0.5	2	0.05	10	1	0.88
		$\bar{x} = 0.96 \times 10^{-10}$; $\sigma = 0.20 \times 10^{-10}$						
Calcium Ca ^a								
AMD	4.6	r	54.8	–	–7.32	r	–	–
GMW	117	2.2×10^{-10}	33.1	15	9.12	40	1.2	0.91
LL	700	1.0×10^{-10}	285.0	3	35.80	6	1	0.76
TARD	365	1.6×10^{-10}	104.0	15	28.90	27	1.3	0.91
		$\bar{x} = 1.6 \times 10^{-10}$; $\sigma = 0.60 \times 10^{-10}$						
Cadmium Cd								
ARD	45	0.89×10^{-10}	11.5	18	3.66	16	1	0.92
GMW	7	0.84×10^{-10}	0.6	80	0.81	110	1.2	0.97
LL	2	0.86×10^{-10}	<0.5	39	0.20	30	1.1	0.99
TARD	12	0.83×10^{-10}	1.9	43	1.31	98	1.3	0.95
		$\bar{x} = 0.86 \times 10^{-10}$; $\sigma = \times 10^{-10}$						
Chloride Cl ^a								
ARD	2000	4.4×10^{-10}	756.0	0	–	–	–	–
GMW	1000	3.8×10^{-10}	362.0	0	–	–	–	–
LL	6000	3.8×10^{-10}	2311.0	0	–	2	1	0.71
TARD	1000	3.6×10^{-10}	367.0	0	–	–	–	–
		$\bar{x} = 3.9 \times 10^{-10}$; $\sigma = 0.35 \times 10^{-10}$						
Copper Cu								
ARD	15	0.70×10^{-10}	2.0	56	1.72	30	1	0.62
LL	1	0.67×10^{-10}	<0.40	25	0.09	60	0.8	0.64
TARD	2	nf	<0.40	–	0.29	123	1	0.69
		$\bar{x} = 0.69 \times 10^{-10}$; $\sigma = 0.21 \times 10^{-11}$						
Iron Fe								
ARD	200	0.93×10^{-10}	21.9	65	23.40	94	1	0.78
GMW	1.5	nf	0.5	–	0.08	nf	–	–
LL	12	0.69×10^{-10}	1.5	47	1.17	700	1.6	0.67
TARD	10	0.87×10^{-10}	2.3	20	0.82	nf	–	–

(continued)

Table 2. (continued)

	(1) Initial concentration, C ₀ (mg/L)	(2) Diffusion coefficient, D (m ² /s)	(3) Porewater concentration, C _{aq} (mg/L)	(4) Linear distribution coefficient, K _d (diffusion) (mL/g)	(5) Total mass retained in GCL (mg)	(6) Distribution coefficient, K(batch) (mL/g)	(7) Freundlich constant, ε	(8) Regression coefficient, R ²
Potassium K ^a		$\bar{x} = 0.83 \times 10^{-10}$; $\sigma = 0.13 \times 10^{-10}$						
ARD	400	3.2×10^{-10}	134.2	5	20.00	5	1	0.87
GMW	12	3.5×10^{-10}	4.9	6	0.65	17	1.9	0.98
LL	190	3.2×10^{-10}	73.1	2	8.54	3	1	0.93
TARD	8	nf	8.8	–	0	5	1.4	0.91
Magnesium Mg ^a		$\bar{x} = 0.33 \times 10^{-10}$; $\sigma = 0.17 \times 10^{-10}$						
ARD	1	r	7.9	–	–0.96	r	–	–
GMW	60	0.86×10^{-10}	19.7	10	4.00	10	1	0.95
LL	244	1.3×10^{-10}	95.2	3.5	10.03	19	1	0.91
TARD	45	1.2×10^{-10}	17.0	6	2.60	16	0.8	0.82
Manganese Mn ^a		$\bar{x} = 1.1 \times 10^{-10}$; $\sigma = 0.23 \times 10^{-10}$						
ARD	23 ¹	0.99×10^{-10}	6.0	10	1.28	3	1	0.87
GMW	1.7	1.0×10^{-10}	0.52	11	<0.01	131	1.1	0.81
LL	7	1.9×10^{-10}	2.78	8	0.53	40	1.2	0.94
TARD	7	0.99×10^{-10}	1.30	31	0.65	92	1.2	0.79
Sodium Na ^a		$\bar{x} = 1.2 \times 10^{-10}$; $\sigma = 0.45 \times 10^{-10}$						
ARD	800	r	692.0	–	–82.0	r	–	–
GMW	776	r	48.3	–	–49.2	r	–	–
LL	2300	r	1388.0	–	–107	r	–	–
TARD	340	r	307.0	–	–37	r	–	–
Nickel Ni								
ARD	17	0.82×10^{-10}	3.60	27	1.62	17	1	0.93
LL	6	0.73×10^{-10}	1.06	34	0.59	59	1	0.88
TARD	6	0.76×10^{-10}	0.94	53	0.66	74	1	0.90
Sulphate SO ₄ ^a		$\bar{x} = 0.77 \times 10^{-10}$; $\sigma = 0.46 \times 10^{-11}$						
ARD ^b	3102	2.2×10^{-10}	1323.0	1.3	119	nf	–	–
GMW	1506	1.1×10^{-10}	677.5	1.3	33.3	nf	–	–
LL	75	nf	41.0	–	1.36	r	–	–
TARD	1290	1.0×10^{-10}	652.0	2.4	58.8	nf	–	–
Strontium Sr		$\bar{x} = 1.4 \times 10^{-10}$; $\sigma = 6.7 \times 10^{-10}$						
GMW	2	1.5×10^{-10}	0.8	8	<0.01	62	0.6	0.90
LL	12	0.92×10^{-10}	4.2	7	0.47	60	0.5	0.95
		$\bar{x} = 1.2 \times 10^{-10}$; $\sigma = 4.1 \times 10^{-11}$						

(continued)

Table 2. (continued)

	(1) Initial concentration, C_0 (mg/L)	(2) Diffusion coefficient, D (m^2/s)	(3) Porewater concentration, C_{aq} (mg/L)	(4) Linear distribution coefficient, K_d (diffusion) (mL/g)	(5) Total mass retained in GCL (mg)	(6) Distribution coefficient, K (batch) (mL/g)	(7) Freundlich constant, ε	(8) Regression coefficient, R^2
Zinc Zn	102	0.80×10^{-10}	31.4	14	8.16	27	1	0.88
ARD	16	0.77×10^{-10}	4.9	17	1.51	57	0.8	0.92
LL	8	0.82×10^{-10}	1.5	31	0.74	64	1.2	0.93
TARD		$\bar{x} = 0.80 \times 10^{-10}; \sigma = 0.25 \times 10^{-11}$						

nf = no good fit by model; r = observed release of ions into solution; blank entry = not calculated owing to loss or no change in mass.

\bar{x} = mean; σ = standard deviation.

^aIon was present in GCL porewater. Initial conditions were modelled in Pollute.

^bDiffusion coefficient determined from receptor reservoir measurements only.

calculated difference between the mass lost/gained in the source and the receptor, that is,

$$[c_{\text{initial}}(\text{source}) - c_{\text{final}}(\text{source})] - [c_{\text{final}}(\text{receptor}) - [c_{\text{initial}}(\text{receptor})]$$

and the porewater concentration (C_{aq} , column 3) reports the constituent's aqueous concentration in mg/L. The K_d values that provided the best fit to the data are reported in column 4 as K_d (diffusion).

The average diffusion coefficients for Cu, Cd, Zn, Fe and Ni covered a narrow range for all waters, from the lowest for Cu in LL of $D = 0.67 \times 10^{-10} m^2/s$ to the highest for Fe of $D = 0.93 \times 10^{-10} m^2/s$ in ARD. As, Al, Mg, Mn and Sr had slightly higher diffusion coefficients (from $D = 0.96 \times 10^{-10} m^2/s$ to $D = 1.2 \times 10^{-10} m^2/s$). Average K, Ca and SO_4 diffusion coefficients ranged from $1.6 \times 10^{-10} m^2/s$ to $3.3 \times 10^{-10} m^2/s$.

Iron diffusion and sorption coefficients showed the most scatter (or larger variance) among different waters. In the case of Fe in GMW, the initial concentration of Fe dropped from 2 mg/L to <0.4 mg/L within the first day, similar to Cu in TARD. The small concentration and high pH probably caused immediate precipitation upon contact with the bentonite. The development of an orange-red ring within the bentonite in the ARD test showed evidence of an Fe oxy-hydroxide precipitate (also observed in Lange et al. 2007a). Consequently, the saturation indices calculated from the ARD porewater were greater than 1 for several iron salts: ferrihydrite (SI = 3.21); gibbsite (SI = 2.75); lepidocrocite (SI = 5.03); and goethite (SI = 5.91). This precipitate provides another mineral surface for metal sorption, in addition to the bentonite.

Figure 6 shows diffusion coefficients measured for different clay/clay-soil mixtures under a laboratory set-up similar to that in this study. The diffusion coefficient for Cl ranged from $3.6 \times 10^{-10} m^2/s$ (TARD) to $4.4 \times 10^{-10} m^2/s$ (ARD) in this study; Lake (2000) reported a diffusion coefficient within this range of $D = 3.75 \times 10^{-10} m^2/s$ for a GCL with similar porosity (and height). The metal diffusion coefficients for the current study plot to the left of the data in Figure 6; however, some similarities between relative ions were noted. For example, Cd diffusion coefficients in this study ranged from $0.83 \times 10^{-10} m^2/s$ for TARD to $0.89 \times 10^{-10} m^2/s$ for ARD, approximately four times less than chloride; Camur and Yazicigil (2005) similarly found that D_e for Cd (in Ankara clay) was 4.5 times less than D_e for Cl.

In addition to the anion Cl, SO_4 also had the highest diffusion coefficient for the ARD water (Table 2). Lake and Rowe (2000) and Petrov et al. (1997) speculated that increases in Cl migration occurring in multicomponent solutions are partly due to double layer and c -axis contraction: this is consistent with the ARD waters having a very high loading of metals (charges +2 and +3) compared with the other solutions. This may also explain why As experienced faster diffusion in the ARD (than in other waters), as it is typically present in anionic form.

Few diffusion data for Ca, Mg or Na have been

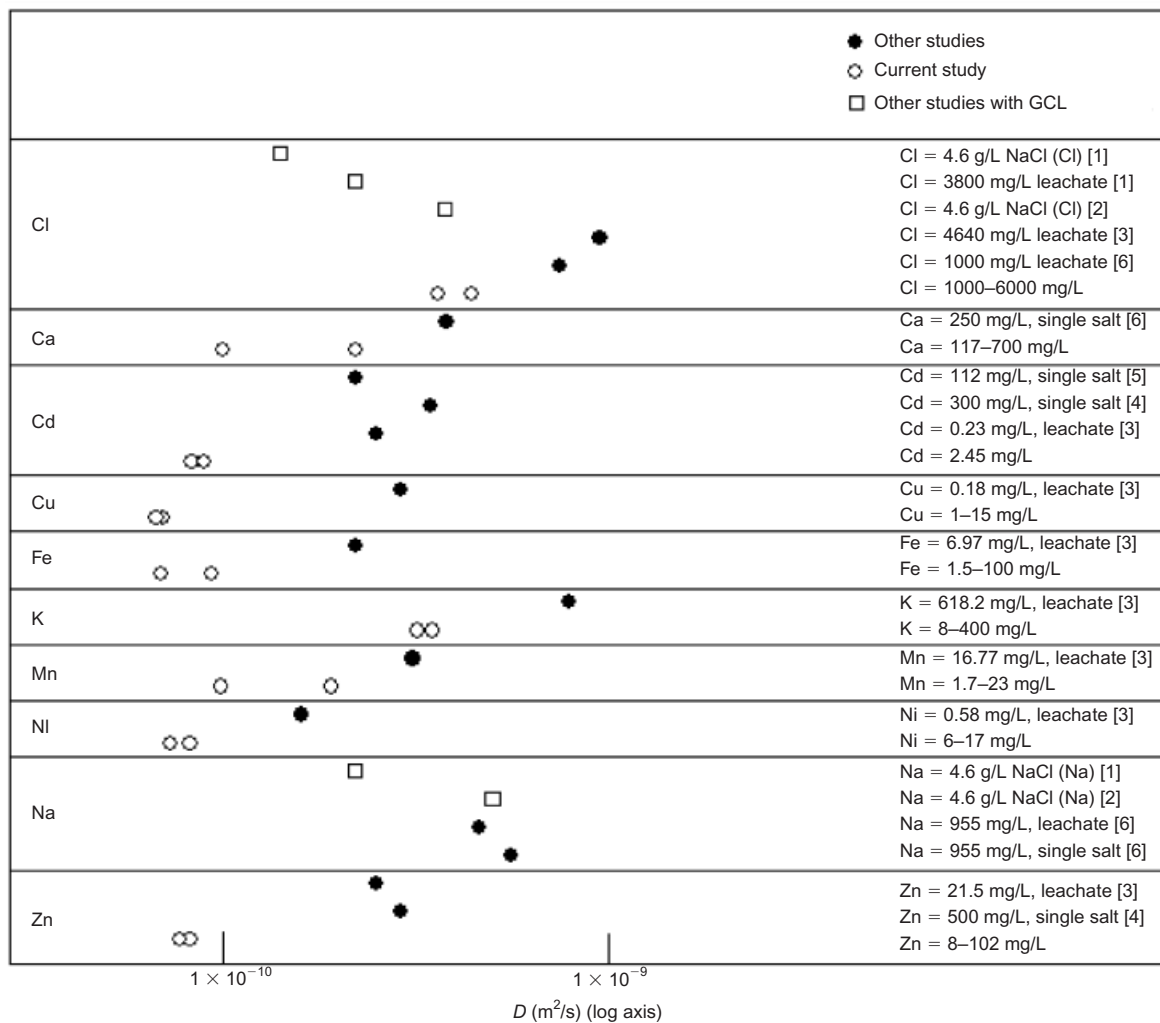


Figure 6. Diffusion coefficients from the literature and the current study. 1: GCL, $H = 7.1$ mm, $n = 0.67–0.70$ (Lake and Rowe 2000). 2: GCL, $H = 11.1$ mm, $n = 0.80$ (Lake and Rowe 2000). 3: Ankara clay, $n_e = 0.45$ (Camur and Yazicigil 2005). 4: Natural clay, $n = 0.43$ (Do and Lee 2006). 5: Clay soil, $n = 0.34$ (Roehl and Czurdza 1998). 6: Undisturbed clayey soil, $n = 0.39$ (Barone *et al.* 1990)

reported, as these ions can experience desorption from clays. For example, Barone *et al.* (1989) showed that Ca was adequately modelled when the solution was composed of a single salt; however, it was ‘not fitted’ when the source solution was an MSW leachate. They indicated that this situation arose because the Ca and Mg originally present on the clay exchange sites were ‘heavily desorbed to accommodate the adsorption of migrating Na, K and possibly NH_4 , causing hardness halo effects’. Hardness halo effects refer to the expelling of Ca and Mg from a soil when in contact with a leachate (e.g. landfill leachate): as a result the concentrations of these cations in the effluent or receptor may become elevated relative to the original source solution.

Calcium diffusion data were adequately fitted by the model for LL, TARD and GMW, and covered a small range from 1.0×10^{-10} m^2/s to 2.2×10^{-10} m^2/s ; however, in the ARD cell an overall release of Ca occurred from the GCL, and the concentration of Ca increased slightly in the source reservoir (as did that of Mg). In addition to exchange mechanisms, Ca concentrations may

have increased in the source reservoir owing to the dissolution of calcite in the bentonite. In fact, this trend was more significant in the case of Na in the ARD water, where Na concentrations in the source reservoir showed a slight increase followed by a very slow decline, while the concentration of Na ions into the receptor reservoir showed a rapid increase. The large release of Na ions into the receptor is probably the result of the high loading rate of metals (specifically in the ARD). However, the reason for the back-diffusion of Na ions into the source reservoir and the subsequent slow movement of Na ions out of the source appears to be twofold: first, the initial presence of Na ions in the receptor reservoir and the bentonite, which reduced the gradient between the source and the receptor; and second, the observed increase in pH in the ARD source reservoir from 2.6 to 5. This increase reflects an upward migration of hydroxide (OH) ions. The free diffusion coefficient for OH is large compared with other ions (Rowe *et al.* 2004), and thus if OH ‘paired’ with Na, Mg or Ca, their overall movement, compared with that of an Na-Cl pair, would be greater, thus retarding the Na

ion's movement from the source. Figure 7 shows the concentrations (mg/L) of SO₄, K and Na for both reservoirs in the ARD cell; the concentration in moles/L of OH ions is shown on the right axis, and was calculated from pH (pOH). The diffusion curve for K was not affected (similar to other solutions) and was adequately represented by the diffusion coefficient $D = 0.10 \times 10^{-10} \text{ m}^2/\text{s}$. A slightly flat source concentration curve for Na was also noted for LL, where OH concentrations also increased slightly in the source.

Al, Na, Ca, Mg, SO₄ and Mn ions were initially present in the bentonite porewater, and diffused into the receptor reservoir during hydration. This influenced the shape of

the curve slightly (Figure 8 for Mn); however, careful modelling of initial boundary conditions allowed for a satisfactory fit to the data. Again, in some cases no fit was possible when significant desorption and/or back-diffusion of such ions occurred.

3.2. Sorption

The level of sorption of metals varies according to their mobility pattern, their interaction with the soil, and their ability to form inorganic/organic complexes. Sorption data from the batch tests can be represented by the Freundlich equation,

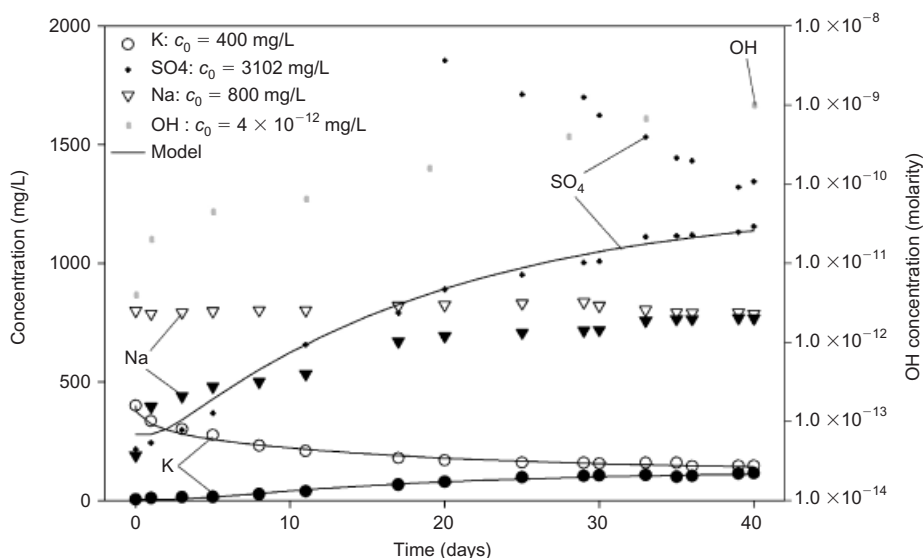


Figure 7. Source and receptor diffusion profiles of Na, SO₄, K and OH for ARD. Symbols concentrations, and lines give the calculated profiles. Closed symbols represent source values, and open symbols show the receptor values

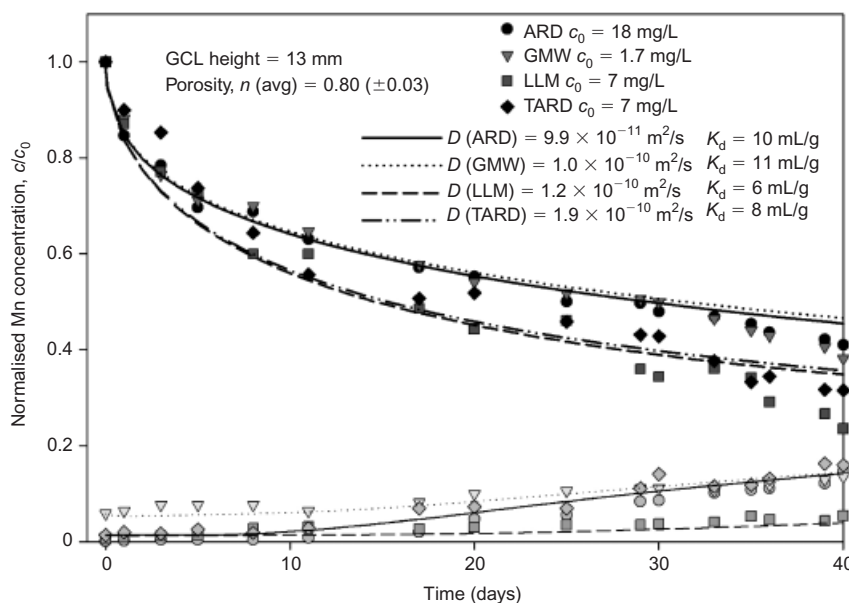


Figure 8. Source and receptor diffusion profiles of Mn for different solutions. Symbols represent the measured concentrations, and lines give the calculated profiles. Closed symbols represent source values, and open symbols show the receptor values

$$\frac{X}{M} = K(\text{batch})C_e^\varepsilon \quad (6)$$

where X/M is the amount of solute retained per unit mass of soil [MM^{-1}], C_e is the equilibrium concentration of solute remaining in solution, and ε is a Freundlich parameter. The special case of $\varepsilon = 1$ corresponds to linear sorption and $K(\text{batch}) = K_d$. The Freundlich parameters $K(\text{batch})$ and ε deduced from the 24 h batch test (columns 6, 7) were obtained based on a best fit from two (duplicate) data sets, and the corresponding R^2 values produced from least squares regression to all the data are given in column 8. In general, K_d values from this study are typically at the low end of K_d values reported in literature. However, it is important to note that those sorption studies use the 'separated' less than 0.2 mm fraction of clay, and essentially deal with pure clay, whereas this study used the bulk bentonite.

The $K_d(\text{diffusion})$ value provided a significantly closer fit to the diffusion data than the partitioning coefficient determined from the batch sorption tests, $K(\text{batch})$. Although some batch sorption data showed non-linear behaviour, indicated by a good fit to the Freundlich equation, the assumption of linearity for K_d did not have a major impact on the results, as the concentration range of interest was typically small, and covered a narrow range. The difference between the batch sorption isotherm and the equivalent isotherm from the diffusion values is illustrated using Cd and Cu from different solutions.

Figure 9 compares batch test isotherms for two selected metals, Cd (GMW) and Cu (ARD), with the equivalent (linear) isotherm from the $K_d(\text{diffusion})$ values. In the case of Cd, the batch sorption test produced a higher K value than did the diffusion test, whereas the opposite occurred for Cu. It is likely that the iron oxyhydroxide formation in the ARD diffusion cell promoted additional Cu retention,

producing a $K_d(\text{diffusion}) > K_d(\text{batch})$ for Cu. Iron oxyhydroxide was probably also responsible for other elements in the ARD, such as Mn and Ni, that also had $K_d(\text{diffusion}) > K_d(\text{batch})$, and this is the focus of a separate study.

With few exceptions, batch tests overestimated sorption: that is, $K_d(\text{batch}) > K_d(\text{diffusion})$. For example, batch tests showed that Al was sorbed to the clay for all waters, whereas the opposite was observed (Al was desorbed) for the diffusion cells LL, GMW and TARD (exception of ARD). The increase in pH observed in the batch sorption tests for LL, GMW and TARD indicates the possible sorption of an aluminium hydroxide. In the ARD diffusion cell, the initial high concentration of the Al in the ARD prevented the Al from desorbing (common ion effect) and created a concentration gradient that promoted sorption and possible surface precipitation. Calculated SI values for ARD porewaters showed that Al could precipitate in the form of an aluminium sulphate salt (SI = 8.55), alunite (SI = 11.45) or boehmite (SI = 2.46).

Most sorption studies have commonly shown that metals experience higher sorption with increasing pH (Yong 2001; Abollino *et al.* 2003; Sen Gupta and Bhattacharyya 2006), and most metal hydroxide, oxide, carbonate and phosphate precipitates form under alkaline conditions (Lindsay 1979). Similarly, the batch tests in this study associated with near-neutral to basic solutions gave higher K_d values. Copper in the TARD water experienced a significant increase in sorption compared with all other waters. The TARD water had the largest pH, and the increase in pH when in contact with the bentonite probably bordered on the sorption edge of Cu, a narrow pH region where metal retention essentially increases from near 0 to near 100% (Benjamin and Leckie 1982).

Although the mobility order for LL, TARD and GMW changed, it was generally consistent with other researchers'

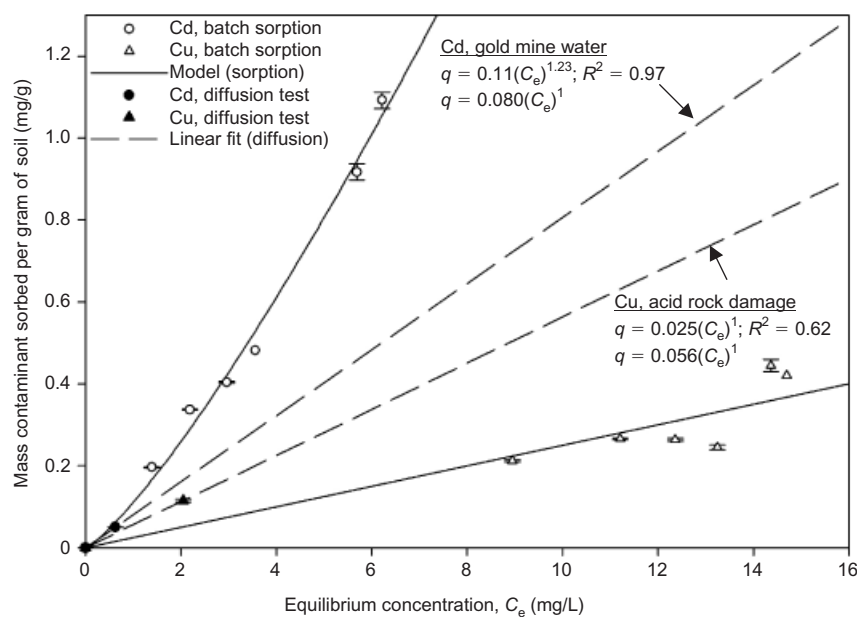


Figure 9. Comparison of sorption data from batch test and diffusion test for Cu and Cd

results, in that Cu and Fe were less mobile, and Cd, Ni and Zn were more mobile. Cadmium isotherm curves for LL, TARD and GM were similar to 'S-type' curves (Giles *et al.* 1974), where initially lower slope values increase with increasing C_e , usually indicative of surface precipitation or cooperative sorption. Alvarez-Puebla *et al.* (2005) showed

similar curves for Co(II) soil sorption at pH values greater than 7. Other researchers have reported higher removal rates at lower initial concentrations of Cd: Sharma and Srivastava (2006) noted a 40% increase in removal by decreasing the concentration of Cd in solution from 2.0×10^{-4} M to $\times 10^{-4}$ M (pH = 6.5, 0.01M ionic strength).

Table 3. Relative percentages of species for trace metals and selected cations for all waters calculated from PHREEQC (Parkhurst and Appelo 1999)

Species	Relative % of species				Species	Relative % of species			
	ARD	GMW	LL	TARD		ARD	GMW	LL	TARD
Aluminium Al					Potassium K				
Al+3	10.6	0.03		5.56	K+	95.11	96.4	99.6	97.1
AlSO ₄ +	82.9	0.22		36.6	KSO ₄ -	4.89	3.61	0.11	2.97
Al(SO ₄) ₂ -	6.51	0.01		1.97	K(acetate)	n/a	n/a	0.05	n/a
AlOH+2				9.79	Magnesium Mg				
Al(OH) ₂ +		19.3		40.5	Mg ⁺²	67.0	70.3	82.9	72.7
Al(OH) ₃		19.9		4.31	MgSO ₄	33.0	28.4	0.71	27.3
Al(OH) ₄ -		60.0	100.0	1.26	MgOH+			12.0	
Arsenic As					MgCO ₃			3.21	
H ₂ AsO ₄ -	77.4	37.3		87.7	MgHCO ₃ +		1.28	0.01	
H ₃ AsO ₄	22.6			0.02	Mg(acetate)+	n/a	n/a	0.77	
HAsO ₄ -2	0.01	62.7	22.1	12.2	Manganese Mn				
AsO ₄ -3		0.01	77.9		Mn+2	76.6	76.3	70.3	77.7
Calcium Ca					MnSO ₄	22.1	21.0	0.24	22.3
Ca+2	61.7	65.2	81.4	68.1	MnCl+	1.20	0.81	1.93	
CaSO ₄	38.3	32.9	0.87	31.9	MnCl ₂	0.06	0.02	0.26	
CaOH+			0.56		MnHCO ₃ +		1.90	0.01	
CaNH ₃ +2			9.38		MnOH+			26.7	
CaHCO ₃ +		1.89			Mn(acetate)+			0.36	
Ca(acetate)+	n/a	n/a	0.61	n/a	Sodium Na			99.61	
CaCO ₃		0.04	5.97		Na+	96.3	97.0	99.6	97.7
Cadmium Cd					NaSO ₄ -	3.75	2.82	0.0800	2.32
Cd+2	22.4	33.6	0.63	64.3	NaHCO ₃		0.17		
CdSO ₄	14.2	17.1	0.01	30.5	NaCO ₃ -			0.28	
Cd(SO ₄) ₂ -2	6.34	4.52		5.11	Na(acetate)	n/a	n/a	0.05	
CdCl ₂	6.35	2.86	1.29		Nickel Ni				
CdCl+	50.5	41.3	4.04		Ni+2	62.5	n/a	0.110	70.8
CdOHCl			82.8		NiSO ₄	33.7	n/a		29.2
CdCl ₃ -	0.26	0.05	0.18		Ni(SO ₄) ₂ -2	0.04	n/a		0.01
Cd(OH) ₂			6.93		NiCl+	3.78	n/a	0.02	
CdCO ₃		0.30	0.66		Ni(OH) ₂		n/a	26.3	
Copper Cu					Ni(OH) ₃ -		n/a	39.3	
Cu+2	60.5	n/a		67.9	Ni(NH ₃) ₂ +2		n/a	28.2	
CuSO ₄	37.5	n/a		31.5	NiNH ₃ +2		n/a	5.27	
CuCl ₂	0.02	n/a			Strontium Sr				
CuCl+	2.03	n/a			Sr+2	n/a	68.4	88.6	n/a
Cu(OH)+				0.62	SrSO ₄	n/a	29.9	0.82	n/a
Cu(OH) ₃ -		n/a	72.2		SrHCO ₃ +	n/a	1.67		n/a
Cu(OH) ₄ -2		n/a	2.25		SrCO ₃	n/a		2.66	n/a
Cu(OH) ₂		n/a	25.0		SrNH ₃ +2	n/a		6.48	n/a
Iron Fe					SrNO ₃ +	n/a		0.29	n/a
Fe+3	6.11				Sr(acetate)+	n/a	n/a	0.61	n/a
FeSO ₄ +	68.4				Zinc Zn				
Fe(SO ₄) ₂ -	12.2				Zn+2	55.0	n/a		66.8
FeCl+2	2.31				ZnSO ₄	32.6	n/a		30.0
FeCl ₂ +	0.22				Zn(SO ₄) ₂ -2	9.39	n/a		3.19
FeOH+2	4.50	0.01		0.05	ZnCl+	2.92	n/a		
Fe(OH) ₂ +	3.32	97.3		99.7	ZnCl ₂	0.16	n/a		
Fe(OH) ₄ -			99.1		ZnCl ₃ -	0.01	n/a		
Fe(OH) ₃		2.64	0.90	0.28	Zn(OH) ₃ -		n/a	76.6	
Fe ₂ (OH) ₂ +4	1.40				Zn(OH) ₄ -2		n/a	12.8	
Fe ₃ (OH) ₄ +5	0.06				Zn(OH) ₂		n/a	10.2	

3.3. Speciation

The presence of complex species in solution can impact on the transport of metals through the GCL as they are variably charged (positive, negative or neutral). Table 3 displays the relative percentages of species present for trace elements and other cations calculated by speciation modelling using PHREEQC Interactive version 2.13.2, with the Minteq v4 database (Parkhurst and Appelo 1999). The model output can provide an estimate of the concentration of free and complexed metals.

Calcium, K, Mn and Na are shown to exist dominantly as free (uncomplexed) metal ions (e.g. Ca^{2+}), and metals such as Al, Cd, Fe, Ni, Cu and Zn show a higher association with the ligands SO_4^{2-} , Cl^- and OH^- . Eighty-three per cent of Al, for example, is complexed with SO_4 in the ARD, and 99% of Al is complexed with hydroxide in the GMW. Cd also showed a higher association with Cl (CdCl^+) than metals such as Cu or Ni. This may help to explain the relative mobility of Cd in comparison with the other metals. At higher pH levels an association with OH and Cl dominates, for example CdOHCl for Cd in TARD. The 97% of Fe present in the form of $\text{Fe}(\text{OH})^{2+}$ for the GMW may explain the rapid precipitation and the inability to measure Fe concentrations for this cell. This can also apply to the LL and TARD solutions, which show that almost all the Fe is present as Fe^{3+} hydrolysed species.

Very few complexes are shown to associate with the organics: acetate complexes constituted less than 1% (total) of overall speciation. This may occur as the model uses only the dissociated ions to calculate associations, and the acids used in the LL are weak acids and therefore have low dissociation constants.

All predominant forms of As were negatively charged for each solution. Arsenic did not show any association with other ions in solution. Batch sorption for As was greatest for ARD where the lower pH environment promoted the positive sorption of anions compared with the other waters.

4. CONCLUSIONS

The diffusive transport of Al, As, Cd, Ca, Cl, Cu, Fe, K, Mg, Mn, Ni, SO_4 , Sr and Zn through GCLs from four waters associated with mining and landfill wastes was investigated. The average diffusion coefficients for As, Cu, Cd, Zn, Fe and Ni ($D = 0.69 \times 10^{-10} \text{ m}^2/\text{s}$ to $D = 0.96 \times 10^{-10} \text{ m}^2/\text{s}$) covered a narrow region for all waters. Al, Mg, Mn and Sr had slightly higher diffusion coefficients ($D = 1.1 \times 10^{-10} \text{ m}^2/\text{s}$ to $D = 1.6 \times 10^{-10} \text{ m}^2/\text{s}$). K, Ca and SO_4 diffusion coefficients ranged from $1.6 \times 10^{-10} \text{ m}^2/\text{s}$ to $3.3 \times 10^{-10} \text{ m}^2/\text{s}$.

The individual metal diffusion coefficients did not change significantly for different solution compositions: for example, D for Ni (Figure 3) ranged from $0.73 \times 10^{-10} \text{ m}^2/\text{s}$ to $0.82 \times 10^{-10} \text{ m}^2/\text{s}$ (average of $0.77 \times 10^{-10} \text{ m}^2/\text{s}$). This suggested that although solution composition had some effect on the metal diffusion coefficient, sorption to the GCL was the dominant control on metal mobility.

The sorption coefficients calculated from the diffusion experiments, K_d (diffusion), provided a much better fit to the diffusion data than did the batch test coefficients, K_d (batch), which tended to overestimate the actual mass retained.

Although different solutions did not have a significant impact on metal migration, other cations were sensitive to the solution pH. In the case of acidic mine drainage (ARD), a significant release of Na ions occurred in the receptor reservoir, and the Na movement out of the source reservoir was retarded by the back-diffusion of OH ions from the pH change and Na ions from the bentonite porewater.

Speciation modelling can be used as a guide to explain certain observed phenomena for both diffusion and sorption of metal ions, as some tend to form complexes while others may appear as negatively charged anions under certain conditions.

Significant attenuation of metals in the GCL was evident from the measured diffusion profiles, where concentrations in the receptor reservoir remained very low for the duration of the test: this helps to confirm earlier work (e.g. Lange *et al.* 2007a) showing that GCLs have potential use as a barrier material for the containment of metal-bearing wastes.

ACKNOWLEDGEMENTS

This work was funded by CRESTech, an Ontario Centre of Excellence, and Terrafix Geosynthetics Inc. and NAUE GmbH & Co. KG. Additional funding was provided by the Natural Sciences and Engineering Research Council of Canada (NSERC). The value of discussion with K. Von Mauberge and B. Herlin is gratefully acknowledged. The XRD quantitative diffraction data analysis was provided by J. Talbot at K/T GeoServices.

NOTATIONS

Basic SI units are given in parentheses.

C_e	batch sorption test equilibrium concentration (M/m^3)
c	solute concentration in solution phase (M/m^3)
c_{s0}	initial contaminant concentration in source solution (M/m^3)
c_{r0}	initial contaminant concentration in the receptor solution (M/m^3)
D	diffusion coefficient (m^2/s)
D_e	effective diffusion coefficient (m^2/s)
D_p	diffusion coefficient based on total porosity as defined by Lake and Rowe (2000) (m^2/s)
Eh	redox potential (mV)
ε	Freundlich parameter (dimensionless)
$f_t(t)$	mass flux of contaminant into clay at time t (Mm^2/s)
h_b	volume of receptor fluid per unit area of sample (m)
H_t	volume of source fluid per unit area of

	sample (i.e. typically height of fluid in reservoir) (m)
K_d	linear distribution coefficient (m^3/M)
K	distribution coefficient; $\varepsilon \neq 1$ (m^3/M)
K_a	acid dissociation constant (dimensionless)
n	soil porosity (dimensionless)
n_e	effective soil porosity (dimensionless)
pe	measure of electron activity (dimensionless)
pH	measure of activity of dissolved hydrogen (dimensionless)
Q_e	batch sorption test amount of constituent removed from solution per gram of bentonite (dimensionless)
q_c	amount of fluid withdrawn from source reservoir per unit area of sample (m^3/s)
t	time (s)
z	distance from contaminant source (m)
ρ	dry density of soil (M/m^3)

ABBREVIATIONS

ARD	acid rock drainage
DDW	deionised deaired water
GCL	geosynthetic clay liner
GMW	gold mine (pore) water
ICP	inductively coupled plasma
LL	landfill leachate
MSW	municipal solid waste
SI	saturation index
TARD	treated acidic rock drainage

REFERENCES

- Abollino, O., Aceto, M., Malandrino, M., Sarzanini, C. & Mentasti, E. (2003). Adsorption of HMs on Na-montmorillonite. *Water Resources*, **37**, No. 7, 1619–1627.
- Alvarez-Puebla, R. A., Garrido, J. J., Valenzuela-Calahorra & C., Goulet, P. J. G. (2005). Retention and induced aggregation of Co(II) on a humic substance: sorption isotherms, infrared absorption, and molecular modeling. *Surface Science*, **575**, No. 1–2, 136–146.
- Artiola-Fortuny, J. & Fuller, W. H. (1982). Humic substances in landfill leachates: I. Humic acid extraction and identification. *Journal of Environmental Quality*, **11**, 663–669.
- Allan, R. J. (1995). Impact of mining activities on the terrestrial and aquatic environment with emphasis on mitigation and remedial measures. *Heavy Metals*, Salomons, W., Forstner, U. and Mader, P., Editors, Springer-Verlag, New York, pp. 120–140.
- Baas-Becking, L. G. M., Kaplan, I. R. & Moore, D. (1960). Limits of the natural environment in terms of pH and oxidation-reduction potentials. *Journal of Geology*, **68**, No. 3, 243–284.
- Barone, F. S., Yanful, E. K., Quigley, R. M. & Rowe, R. K. (1989). Effect of multiple contaminant migration on diffusion and adsorption of some domestic waste contaminants in a natural clayey soil. *Canadian Geotechnical Journal*, **26**, No. 2, 189–198.
- Barone, F. S., Rowe, R. K. & Quigley, R. M. (1990). Laboratory determination of chloride diffusion coefficients in an intact shale. *Canadian Geotechnical Journal*, **27**, No. 2, 177–184.
- Barroso, M., Touze-Foltz, N. von Maubeuge, K. & Pierson, P. (2006). Laboratory investigation of flow rate through composite liners consisting of a geomembrane, a GCL and a soil liner. *Geotextiles and Geomembranes*, **24**, No. 3, 139–155.
- Benjamin, M. M. & Leckie, J. O. (1982). Effects of complexation by Cl, SO₄ and S₂O₃ on adsorption behavior of Cd on oxide surfaces. *Environmental Science and Technology*, **16**, No. 3, 162–170.
- Bouazza, A. & Vangpaisal, T. (2006). Laboratory investigation of gas leakage rate through a GM/GCL composite liner due to a circular defect in the geomembrane. *Geotextiles and Geomembranes*, **24**, No. 2, 110–115.
- Bouazza, A. & Vangpaisal, T. (2007). Gas transmissivity at the interface of a geomembrane and the geotextile cover of a partially hydrated geosynthetic clay liner. *Geosynthetics International*, **14**, No. 5, 316–319.
- Bouazza, A., Jeffèris, S. & Vangpaisal, T. (2007). Investigation of the effects and degree of calcium exchange on the Atterberg limits and swelling of geosynthetic clay liners when subjected to wet–dry cycles. *Geotextiles and Geomembranes*, **25**, No. 3, 170–185.
- Bourg, A. C. M. (1995). Speciation of heavy metals in soils and groundwater and implications for their natural and provoked mobility. *Heavy Metals*, Salomons, W., Forstner, U. and Mader, P., Editors, Springer-Verlag, New York, pp. 19–31.
- Brookins, D. G. (1988). Eh–pH diagrams for geochemistry. *Geochimica et Cosmochimica Acta*, **53**, No. 3, 763.
- Camur, M. Z. & Yazicigil, H. (2005). Laboratory determination of multicomponent effective diffusion coefficients for heavy metals in a compacted clay. *Turkish Journal of Earth Sciences*, **14**, 91–103.
- Chen, M. & Ma, L. Q. (2001). Comparison of three aqua regia digestion methods for twenty Florida soils. *Soil Science Society of America Journal*, **65**, 491–499.
- Dickinson, S. & Brachman, R. W. I. (2006). Deformations of a geosynthetic clay liner beneath a geomembrane wrinkle and coarse gravel. *Geotextiles and Geomembranes*, **24**, No. 5, 285–298.
- Do, N. Y. & Lee, S. R. (2006). Temperature effect on migration of Zn and Cd through natural clay. *Environmental Monitoring and Assessment*, **118**, No. 1–3, 267–291.
- Doner, H. E. (1978). Chloride as a factor in mobilities of Ni(II), Cu(II) and Cd(II). *Soil Science Society of America Journal*, **42**, 882–885.
- EPA Method 9081 (1986). *Cation Exchange Capacity of Soils (Sodium Acetate)*. USEPA, Washington, D. C., USA.
- Feng, D., Aldrich, C. & Ta, H. (2000). Treatment of acid mine water by use of heavy metal precipitation and ion exchange. *Minerals Engineering*, **13**, No. 6, 623–642.
- Frost, R. R. & Griffin, R. A. (1977). Effect of pH on adsorption of arsenic and selenium from landfill leachate by clay minerals. *Soil Science Society of America Journal*, **41**, 53–57.
- Farquhar, G. J. & Rovers, F. A. (1973). Gas production during refuse decomposition. *Water, Air and Soil Pollution*, **2**, 473–495.
- Giles, C. H., Smith, D. & Huitson, A. (1974). A general treatment and classification of the solute adsorption isotherms. *Journal of Colloid and Interface Science*, **47**: 755–765.
- Griffin, R. A. & Shimp, N. F. (1976). Effect of pH in exchange-absorption or precipitation of Pb from landfill leachates by clay minerals. *Environmental Science and Technology*, **10**, No. 3, 1256–1261.
- Jungnickel, C., Smith, D. & Fityus, S. (2004). Coupled multi-ion electrodiffusion analysis for clay soils. *Canadian Geotechnical Journal*, **41**, No. 2, 287–298.
- Kaoser, S., Barrington, S., Elektorowicz, M. & Wang, Li (2005). Effect of Pb and Cd on Cu adsorption by sand-bentonite liners. *Canadian Journal of Civil Engineering*, **32**, 241–249.
- Katsumi, T., Ishimori, H., Onikata, M. & Fukagawa, R. (2008). Long-term barrier performance of modified bentonite materials against sodium and calcium permeant solutions. *Geotextiles and Geomembranes*, **26**, No. 1, 14–30.
- Knox, R. C. & Canter, L. W. (1996). Prioritization of ground water contaminants and sources. *Water, Air and Soil Pollution*, **88**, No. 3–4, 205–226.
- Kolstad, D. C., Benson, C. H., Edil, T. B. & Jo, H. Y. (2004). Hydraulic conductivity of a dense prehydrated GCL permeated with aggressive inorganic solutions. *Geosynthetics International*, **11**, No. 3, 233–240.
- Kozaki, T., Saito, N., Fujishima, A., Sato, S. & Ohashi, H. (1998).

- Activation energy for diffusion of chloride ions in compacted sodium montmorillonite. *Journal of Contaminant Hydrology*, **35**, No. 1–3, 67–75.
- Lake, C. B. & Rowe, R. K. (2000). Diffusion of sodium and chloride through geosynthetic clay liners. *Geotextiles and Geomembranes*, **18**, No. 2, 103–131.
- Lake, C. B., Cardenas, G., Goreham, V. & Gagnon, G. A. (2007). Aluminium migration through a geosynthetic clay liner. *Geosynthetics International*, **14**, No. 4, 201–210.
- Lange, K., Rowe, R. K. & Jamieson, H. J. (2007a). Metal retention in geosynthetic clay liners following permeation by different mining solutions. *Geosynthetics International*, **14**, No. 3, 178–187.
- Lange, K., Rowe, R. K., Jamieson, H. J. & Flemming, R. L. (2007b). Mineral characterization in geosynthetic clay liners using micro-X-ray diffraction. *Proceedings of the 60th Canadian Geotechnical Conference, Ottawa Geo 2007*, pp. 1881–1887.
- Lindsay, W. L. (1979). *Chemical Equilibria in Soils*, John Wiley & Sons, New York, 449 pp.
- Lobo, V. M. M. & Quaresma, J. L. (1990). Diffusion coefficients in aqueous solutions of cadmium chloride at 298 K. *Electrochimica Acta*, **34**, No. 9, 1433–1436.
- Merian, E. (1991). *Metals and their Compounds in the Environment: Occurrence Analysis and Biological Relevance*, UCH, Weintraim/ New York, 1438 pp.
- Müller, W., Jakob, I., Seeger, S. & Tatzky-Gerth R. (2008). Long-term shear strength of geosynthetic clay liners. *Geotextiles and Geomembranes*, **26**, No. 2, 130–144.
- Olsta, J. & Friedman, J. (2002). GCLs in mining remediation and reclamation. *Geotechnical Fabrics Report*, Jan/Feb, 26–29.
- Parkhurst, D. L. & Appelo, C. A. J. (1999). *User's Guide to PHREEQC, Version 2*, PHREEQC Interactive, US Geological Survey.
- Petrov, R. J., Rowe, R. K. & Quigley, R. M. (1997). Selected factors influencing GCL hydraulic conductivity. *Journal of Geotechnical and Geoenvironmental Engineering*, **123**, No. 8, 683–695.
- Reddi, L. N. & Inyang, H. I. (2000). *Geoenvironmental Engineering: Principles and Applications*, Marcel Dekker, New York, 494 pp.
- Roehl, K. E. & Czurda, K. (1998). Diffusion and solid speciation of Cd and Pb in clay liners. *Applied Clay Science* <http://www.ingentaconnect.com/content/els/01691317;jsessionid=2fvjgst7tb36f.victoria>, **12**, No. 5, 387–402.
- Rowe, R. K. & Booker, J. R. (2005). *POLLUTEv7: Pollutant Migration through a Nonhomogeneous Soil*. Distributed by GAEA Environmental Engineering Ltd, Ontario, Canada.
- Rowe, R. K., Lake, C. B. & Petrov, R. J. (2000). Apparatus and procedures for assessing inorganic diffusion coefficients for geosynthetic clay liners. *Geotechnical Testing Journal*, **23**, No. 2, 206–214.
- Rowe, R. K., Quigley, R. M., Brachman, R. W. I. & Booker, J. R. (2004). *Barrier Systems for Waste Disposal Facilities*, Spon Press, London, 587 pp.
- Rowe, R. K., Mukunoki, T., Bathurst, R. J., Rimal, S., Hurst, P. & Hansen, S. (2007). Performance of a geocomposite liner for containing Jet A-1 spill in an extreme environment. *Geotextiles and Geomembranes*, **25**, No. 2, 68–77.
- Saidi, F., Touze-Foltz, N. & Goblet, P. (2006). 2D and 3D numerical modelling of flow through composite liners involving partially saturated GCLs. *Geosynthetics International*, **13**, No. 6, 265–276.
- Schuster, E. (1991). The behavior of mercury in soil with special emphasis on complexation and adsorption processes: a review of the literature. *Water, Air, & Soil Pollution* <http://www.springerlink.com/content/100344/>, **56**, No. 1, 667–680.
- Sen Gupta, S. & Bhattacharyya, K. G. (2006). Removal of Cd(II) from aqueous solution by kaolinite, montmorillonite and their poly(oxo zirconium) and tetrabutylammonium derivatives. *Journal of Hazardous Materials*, **128**, No. 2–3, 247–257.
- Sharma, Y. C. & Srivastava, V. (2006). Adsorption of Cd(II) from aqueous solutions by indigenous clay minerals. *Indian Journal of Chemical Technology*, **13**, No. 3, 218–221.
- Southen, J. M. & Rowe, R. K. (2007). Evaluation of the water retention curve for geosynthetic clay liners. *Geotextiles and Geomembranes*, **25**, No. 1, 2–9.
- Take, W. A., Chappel, M. J., Brachman, R. W. I. & Rowe, R. K. (2007). Quantifying geomembrane wrinkles using aerial photography and digital image processing. *Geosynthetics International*, **14**, No. 4, 219–227.
- Touze-Foltz, N. & Barroso, M. (2006). Empirical equations for calculating the rate of liquid flow through GCL-geomembrane composite liners. *Geosynthetics International*, **13**, No. 2, 73–82.
- Touze-Foltz, N., Duquennoi, C. & Gaget, E. (2006). Hydraulic and mechanical behavior of GCLs in contact with leachate as part of a composite liner. *Geotextiles and Geomembranes*, **24**, No. 3, 188–197.
- Urase, T., Salequzzaman, M., Kobayashi, S., Matsuo, T., Yamamoto, K. & Suzuki, N. (1997). Effect of high concentration of organic and inorganic matters in landfill leachate on the treatment of heavy metals in very low concentration level. *Water Science and Technology*, **36**, No. 12, 349–356.
- Yong, R. N. (2001). *Geo-environmental Engineering*, 1st Edition, CRC Press, Boca Raton, FL, 295 pp.
- Zhang, H., Kamon, M. & Katsumi, T. (2004). Effect of acid buffering capacity on the long-term mobility of heavy metals in clay liner. *Soils and Foundations*, **44**, No. 6, 111–120.

The Editor welcomes discussion on all papers published in *Geosynthetics International*. Please email your contribution to discussion@geosynthetics-international.com by 15 August 2009.